Acta Cryst. (1999). A**55**, 471–479

Quantitative zone-axis convergent-beam electron diffraction (CBED) studies of metals. I. Structure-factor measurements

M. Saunders,[a]*† A. G. Fox[a] and P. A. Midgley[b]

[a]*Center for Materials Science and Engineering, Department of Mechanical Engineering, Naval Postgraduate School, Monterey, CA 93943, USA, and* [b]*Department of Materials Science and Metallurgy, University of Cambridge, Pembroke Street, Cambridge, CB2 3QZ, England. E-mail: martin.saunders@angstrom.uu.se*

(*Received 11 May 1998; accepted 30 September 1998*)

Abstract

The zone-axis CBED pattern-matching technique ZAPMATCH [Bird & Saunders (1992). *Ultramicroscopy*, **45**, 241–251] has been applied to low-order structure-factor measurements in nickel and copper. Considerable disagreement exists between previously published results obtained with a variety of solid-state theories and experimental techniques. The nickel ZAPMATCH results confirm previous electron-diffraction critical-voltage measurements and are in excellent agreement with FLAPW (full-potential linearized augmented plane-wave) theory calculations. This is further proof of the accuracy achievable with ZAPMATCH analysis. For copper, however, while the results support the findings of previous experimental measurements, they are consistently higher than those given by a range of solid-state theories, perhaps demonstrating some limitation in the existing theory. Two extensions to the ZAPMATCH technique are also considered. First, rules are developed to determine the number of structure factors that can be refined accurately from a given CBED pattern. Second, the imaginary potential generally introduced to account for the effects of thermal diffuse scattering (TDS) is also refined. It is shown that, while the widely used Einstein model is a useful approximation, the refined values are consistently higher than the model predicts. In addition, the importance of a second-order (real) TDS correction arising from the Einstein model is investigated. Although its effects are limited in this instance, it may prove to be more significant at lower beam energies or for materials of higher atomic number.

1. Introduction

Since its introduction in the late 1930s (Kossel & MÎllenstedt, 1938), convergent-beam electron diffraction (CBED) has been used to great effect in the solution of a variety of materials problems. For example, point- and space-group information can be deduced from the symmetry of zone-axis patterns (Tanaka, 1989). Lattice parameters, and hence strain, can be investigated using the positions of high-order Laue-zone (HOLZ) deficiency lines (Zuo, 1992). Sample thicknesses can be measured from the interference-fringe spacings in two-beam patterns (Spence & Zuo, 1992). What these techniques have in common is that they all rely on the positions of features in the CBED pattern. However, the nature of CBED has altered considerably in recent years, with greater emphasis being placed on the quantitative analysis of the diffracted intensities.

There are many reasons for this shift towards quantification. First, CBED simulations have advanced to the stage where the effects of elastic scattering [and to a limited extent thermal diffuse scattering (TDS)] can be included with high accuracy. Second, increasing computer power has considerably reduced the time required to perform these simulations. Finally, and perhaps most importantly, energy filters have been introduced into transmission electron microscopes (TEMs), which allows minimization of the contribution of inelastic scattering to the recorded diffraction pattern. This is an essential step as the simulations are (as yet) unable to model the effects of plasmon scattering, core-loss excitations or other inelastic processes at a quantitative level. Thus, the exclusion of such effects from the experimental data considerably enhances the prospects for quantitative comparisons between theory and experiment.

Two alternative strategies have been proposed based on the iterative refinement of CBED simulations until a best fit is obtained between theory and an experimental pattern. Spence & Zuo (1992) have exploited the heightened sensitivity of a close-to systematic diffraction geometry to refine the first- and (sometimes) second-order structure factors representing scattering along the systematic row. Bird & Saunders (1992) opted for a zone-axis geometry in which a two-dimensional set of low-order structure factors can be refined from a single pattern. Both techniques have been demonstrated to provide low-order structure-factor measurements with sufficient accuracy to investigate bonding effects in

† Present address: Analytical Materials Physics, The Ångström Laboratory, Uppsala University, Box 534, 75121 Uppsala, Sweden.

ISSN 0108-7673

crystalline materials (see, for example, Holmestad *et al.*, 1995; Saunders *et al.*, 1995). It must be realized, however, that these quantitative CBED techniques are still in their developmental stage and that more research is required to understand fully the potential of these methods.

In this paper, we present the first application of the zone-axis pattern-matching (ZAPMATCH) technique of Bird & Saunders (1992) to the refinement of low-order structure factors in metals. In previous work (for example, Saunders *et al.*, 1995), ZAPMATCH has been applied with great success to the study of bonding effects in silicon. This is an ideal test material as it can be grown as large perfect (strain-free) crystals, which produce high-quality CBED data. The metals nickel and copper provide a more rigorous test of the technique as the polycrystalline foils are more susceptible to strain and, as such, represent a less-idealized system. In addition, the charge redistribution arising from metallic bonding will be less pronounced than in covalently bonded silicon, allowing us to investigate the sensitivity of the technique to bonding modifications. The precise values of the low-order structure factors in nickel and copper have, in fact, been the subject of much debate with considerable disagreement between solid-state-theory predictions and the results of various experimental techniques [see the paper by Mackenzie & Mathieson (1992) for a review of copper structure-factor measurements, and that by Wang & Callaway (1977) for examples of nickel structure-factor measurements and calculations]. In principle, ZAPMATCH should be more accurate than previous experimental techniques. Thus, we may be able to clarify the situation by comparing our results with previously published values.

We have already stated that quantitative CBED is still a developing technique. In an attempt to add to our understanding, we have addressed three major issues while carrying out our data analysis. First, can a generally applicable method be found to decide how many structure factors can be refined from a specific data set? This is important as previous studies suggest that attempts to recover too much information result in a marked loss in accuracy (Saunders *et al.*, 1999). Second, the simulations include imaginary corrections to the scattering potential, to account for the effects of thermal diffuse scattering (TDS), which are also refined as part of the analysis. Previously, the refined values were ignored as they failed to demonstrate the consistency shown by the charge-related component of the potential. Here we compare the refined values to those given by the Einstein model (Bird & King, 1990) to see if any information can be extracted from them. Third, the theory that produces the imaginary TDS correction potential can also be used to generate real higher-order corrections which could interfere with our structure-factor measurements (Anstis, 1996). In this paper, Anstis (1996) suggests that ZAPMATCH may be capable of making measurements of the second-order correction terms. We have investigated this by repeating our analysis both with and without the use of second-order TDS corrections.

2. CBED pattern-matching techniques

The crystal charge density $\rho(\mathbf{r})$ is related to the electron scattering potential $V(\mathbf{r})$ by Poisson's equation (Saunders *et al.*, 1995). The periodic nature of the scattering potential enables it to be written as a Fourier series,

$$V(\mathbf{r}) = \sum_g V_g \exp(i2\pi\mathbf{g}\cdot\mathbf{r}), \tag{1}$$

where the V_g are loosely referred to as electron 'structure factors' and $\mathbf{g}$ is a reciprocal-lattice vector. To incorporate the effects of the temperature-dependent vibrations of the atoms, we introduce an exponential term $\exp(-Bs^2)$, where $s = \sin\theta/\lambda = g/2$. B will be referred to as the Debye–Waller factor in this paper though this name is often given to the entire exponential term. Thus, the scattering potential is written

$$V(\mathbf{r}) = \sum_g V_g \exp(i2\pi\mathbf{g}\cdot\mathbf{r}) \exp(-Bs^2). \tag{2}$$

The intensities in the diffraction pattern are a complex function of the structure factors describing the scattering potential. The basic principle of most quantitative CBED structure-factor-measurement techniques is that by adjusting these structure factors a best fit between a theoretical simulation and a set of experimental diffracted intensities can be found. The goodness-of-fit between theory and experiment is calculated using a χ^2 expression, for example,

$$\chi^2 = \frac{1}{N_{\text{data}}} \sum_i \frac{(I_i^{\text{ex}} - cI_i^{\text{th}} - I^{\text{back}})^2}{\sigma_i^2}, \tag{3}$$

where I^{ex} are the experimental intensities, I^{th} are the calculated intensities, I^{back} are a set of background intensity levels, c is a normalization constant, σ^2 is the statistical variance of the experimental data and the sum is over all N_{data} intensities (see Saunders *et al.*, 1995, for more details).

The many-beam formalism used for the CBED simulations involves a parameterized form of the scattering potential, $U(\mathbf{r})$, such that

$$U(\mathbf{r}) = \frac{2m_0\gamma}{\hbar^2} V(\mathbf{r}), \tag{4}$$

where m_0 is the rest mass of the electron and γ is the relativistic correction factor.

Approximate values for the structure factors can be calculated by assuming that the atoms are neutral (Doyle & Turner, 1968); however, there will be modifications to these values as a result of the bonding charge redistribution. The greatest changes are observed in the low-order (low-spatial-frequency) structure factors. It is

also these low-order terms that generally dominate the contrast mechanisms in a CBED pattern and to which the data will be most sensitive. The quantitative CBED techniques are therefore based on the premise that the higher-order structure factors can be fixed at their neutral-atom values, while a small set of low-order structure factors is adjusted to obtain the best fit between theory and experiment. The choice of the number of variable structure factors is dependent on the choice of diffraction geometry and sample thickness. The number of fixed higher-order terms is determined by the requirement that the scattering potential used for the simulations is suitably converged. Other variables in the fit include the sample thickness and the various normalization and background constants. Conventionally, Debye–Waller factors are not allowed to vary during the fit as it is difficult to de-couple the effects of bonding from those of variation of the Debye–Waller factor.

3. How many structure factors can be refined?

The choice of the number of structure factors to refine from any given CBED pattern is an important one. We must ensure that only those structure factors to which the data are sensitive are allowed to vary in the pattern-matching calculation. If too many are varied then we can expect a subsequent loss in accuracy as the refinement acquires too much freedom to find a local solution in which the best-fit structure factors are not a true reflection of the actual charge distribution in the crystal. Conversely, if too few are varied then we will be forcing some structure factors to which the data has some sensitivity to remain fixed at their neutral-atom values (see §2). The resultant loss of bonding information from these fixed structure factors can then lead to the remaining variable structure factors compensating from the lost bond charge from the fixed terms. Thus, it is evident that an incorrect choice of the number of variables can produce inaccurate values for the refined structure factors.

The diffraction geometry and sample thickness combine to dictate the number of structure factors to which the data will show sufficient sensitivity for us to include them as variables in the fitting calculations. The geometry defines which reflections will be excited by satisfying their respective Bragg conditions. The sample thickness controls the level of interaction between the incident beam and the scattering potential and, hence, the sensitivity of the data to the various structure factors corresponding to the excited reflections.

Fig. 1 shows an elastic filtered nickel ⟨110⟩ zone-axis CBED pattern acquired at room temperature for a sample of thickness ∼1300 Å. In the zone-axis geometry, the intensities of the low-order reflections decay as a function of the scattering angle. Thus, in our ⟨110⟩ zone-axis patterns, only intensities of the (000), {111} and {200} reflections lie above the background noise level and the data set used for the pattern matching only considers intensities from these reflections. The sensitivity of the data will be biased towards structure factors corresponding to low-angle scattering for which the scattering probabilities should be highest. However, the restricted angular range emphasises this sensitivity imbalance as the {111} and {200} dark-field reflections will be particularly sensitive to their associated structure factors. While the bright-field reflection will show sensitivity to all structure factors, the sensitivity to higher-order structure factors in the dark-field reflections can only arise through multiple scattering with a consequently lower scattering probability. Thus, it should be possible to refine the {111} and {200} structure factors from data acquired from relatively thin samples for which single scattering dominates, whereas thicker samples will be required for the refinement of the higher-order structure factors where multiple scattering is required to boost the sensitivity to these terms.

The sensitivity as a function of the sample thickness has been investigated by carrying out repeated pattern-matching calculations for two room-temperature nickel ⟨110⟩ zone-axis patterns acquired from samples of 800 and 1400 Å thicknesses. An initial fit is carried out in which only the {111} structure factor is allowed to vary (note that the sample thickness, normalization constant and background terms are always included as variables). The fit is then repeated five times, each time with an additional structure-factor variable, until all structure factors out to {400} are refined. Bonding modifications to the low-order structure factors are known to be small

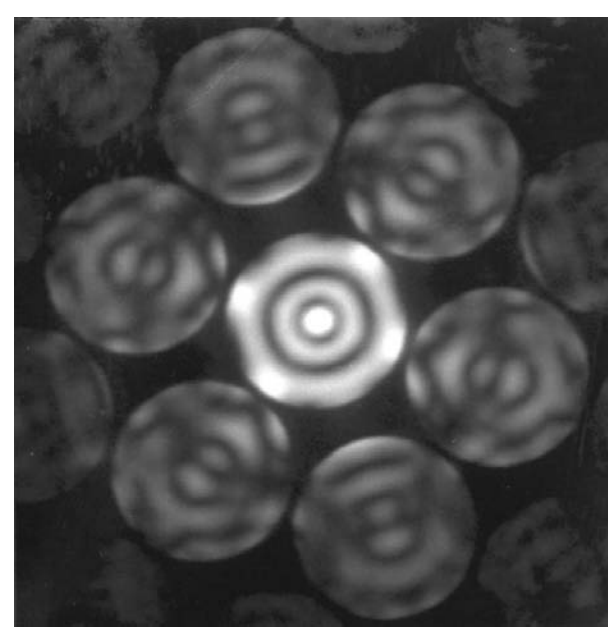

Fig. 1. Elastic filtered nickel ⟨110⟩ zone-axis CBED pattern acquired at room temperature for a sample thickness ∼1300 Å.

Table 1. *Best-fit X-ray structure factors (e atom^{-1}) (top half) and TDS imaginary electron structure-factor corrections (Å^{-2}) (bottom half) for sensitivity tests on room-temperature data for nickel of thickness 800 Å*

g	Fit 1	Fit 2	Fit 3	Fit 4	Fit 5	Fit 6
111	20.48	20.47	20.47	20.47	20.49	20.48
200	–	19.14	19.13	19.14	19.13	19.13
220	–	–	15.47	15.45	15.66	15.68
113	–	–	–	13.65	13.82	13.37
222	–	–	–	–	13.03	13.27
400	–	–	–	–	–	12.82
111	−0.23	−0.22	−0.22	−0.22	−0.22	−0.22
200	–	−0.17	−0.17	−0.19	−0.18	−0.19
220	–	–	−0.14	−0.11	−0.18	−0.18
113	–	–	–	−0.09	−0.08	−0.07
222	–	–	–	–	+0.02	0.00
400	–	–	–	–	–	−0.14

Table 2. *Best-fit X-ray structure factors (e atom^{-1}) (top half) and TDS imaginary electron structure-factor corrections (Å^{-2}) (bottom half) for sensitivity tests on room-temperature data for nickel of thickness 1400 Å*

g	Fit 1	Fit 2	Fit 3	Fit 4	Fit 5	Fit 6
111	20.43	20.46	20.46	20.46	20.46	20.46
200	–	19.12	19.12	19.12	19.13	19.13
220	–	–	15.47	15.47	15.54	15.52
113	–	–	–	13.66	13.62	13.62
222	–	–	–	–	12.90	12.87
400	–	–	–	–	–	11.33
111	−0.23	−0.22	−0.21	−0.21	−0.21	−0.21
200	–	−0.17	−0.19	−0.18	−0.18	−0.18
220	–	–	−0.16	−0.18	−0.18	−0.19
113	–	–	–	−0.15	−0.14	−0.13
222	–	–	–	–	−0.11	−0.12
400	–	–	–	–	–	−0.15

and reduce as a function of the scattering angle. Thus, the additional structure factor introduced as a variable in the fit is expected to deviate little from the neutral-atom value at which it was fixed in the previous fit. By monitoring the variation in the results as we introduce the additional variables, we should be able to detect the point at which sensitivity is lost, *i.e.* introducing structure factors to which the data are insensitive will give the fit too much freedom, producing significant changes in the best-fit structure factors from one fit to the next.

The real and imaginary components of the best-fit structure factors for the successive fits are shown in Tables 1 and 2. It is evident that the 800 Å data (Table 1) show a clear loss in sensitivity upon the introduction of the {222} structure factor as a variable (fit 5). This is reflected by the two highest-order structure factors from the previous fit changing significantly on the introduction of the new variable. This effect can be observed in both the real and imaginary structure factors (shown in the top and bottom halves of Table 1, respectively). The data from the thicker sample (Table 2), however, maintain reasonable sensitivity out to the inclusion of the {400} structure factor (fit 6). Despite this improved sensitivity, the accuracy of the {113}, {222} and {400} structure-factor measurements is still insufficient to determine their bonding contributions. However, for other possible applications of quantitative CBED, such as accurate atom-position refinement (Holmestad *et al.*, 1997), this improved accuracy could prove sufficient.

4. Structure-factor measurements for nickel

⟨110⟩ zone-axis CBED data have been acquired from the same electropolished polycrystalline nickel foil at both room temperature and under liquid-nitrogen cooling. The data were acquired using a Gatan imaging filter (GIF) attached to a Hitachi HF2000 FEG-TEM at the University of Bristol, England. The energy-selecting slit of the GIF was set to a width of 6 eV, centred on the zero-loss energy to produce elastically filtered patterns. The microscope accelerating voltage has been determined to be 198.2 (2) kV from HOLZ deficiency-line positions using a silicon standard. Structure-factor refinements have been carried out for four room-temperature data sets and seven data sets acquired at liquid-nitrogen temperatures, with sample thicknesses ranging from 600 to 2600 Å. The patterns were selected for analysis based on the quality of the pattern symmetry when compared with the 2*mm* symmetry expected at this zone axis. As discussed in §3, intensities for the pattern-matching calculations were extracted from the seven low-order reflections out to {200}.

The simulations include 99 beams in an exact solution of the many-beam equations and a further 246 as Bethe potentials, with each fit taking approximately 10 h. Debye–Waller factors at both temperatures are obtained directly from the refinement calculations as discussed by Saunders *et al.* (1999). The room-temperature Debye–Waller factor varies from 0.31 to 0.35 Å^2 for the different data sets. The liquid-nitrogen Debye–Waller factor varies from 0.13 to 0.17 Å^2. In all the analyses, the major source of error is assumed to be uncertainty in the Debye–Waller factor, which is taken as ±0.02 Å^2 at both temperatures. The electron structure factors obtained from the fits are converted to X-ray structure factors using the Mott formula and the final results are a statistical average of those from the various data sets.

The results for the room-temperature nickel data are shown in Table 3. Column 2 contains the neutral-atom starting values as given by the *ATOM* program of Bird & King (1990) based on the parameterization of Doyle & Turner (1968). Columns 3, 4, 6 and 7 list previously published values obtained using other techniques, such as solid-state theories, X-ray diffraction studies and electron diffraction critical-voltage (CV) measurements. Column 5 contains values that we have obtained using the *WIEN*95 solid-state-theory programs of Blaha *et al.*

Table 3. *Comparison of ZAPMATCH measurements of room-temperature nickel structure factors (e atom^{-1}) with previous theoretical and experimental results*

		Theory			X-ray	CV	
g	Neutral-atom value	Wang & Callaway (1977)	Wakoh & Yamashita (1971)	*WIEN*95	Diana *et al.* (1969)	Fox & Fisher (1988)	ZAPMATCH (average)
111	20.54	20.45	20.28	20.45	20.10 (16)	20.45 (1)	20.47 (2)
200	19.25	19.11	19.05	19.12	18.55 (16)	19.12 (2)	19.13 (2)
220	15.53	15.43	15.35	15.48	15.34 (12)	–	15.43 (8)
113	13.66	13.61	13.47	13.66	–	–	13.67 (8)

Table 4. *Comparison of ZAPMATCH measurements of liquid-nitrogen-temperature nickel structure factors (e atom^{-1}) with previous theoretical and experimental results*

		Theory	CV	
g	Neutral-atom value	*WIEN*95	Fox & Fisher (1988)	ZAPMATCH (average)
111	20.53	20.43	20.44 (1)	20.46 (2)
200	19.23	19.10	19.10 (2)	19.10 (2)
220	15.51	15.46	–	15.44 (3)
113	13.64	13.63	–	13.63 (8)

Table 5. *Comparison of ZAPMATCH measurements of TDS imaginary electron structure factors (Å^{-2}) for nickel at room and liquid-nitrogen temperatures with those given by the Einstein model*

	Room temperature		Liquid-nitrogen temperature	
g	ZAPMATCH	Einstein model	ZAPMATCH	Einstein model
111	−0.21 (1)	−0.16	−0.13 (1)	−0.10
200	−0.19 (1)	−0.15	−0.11 (1)	−0.10
220	−0.15 (2)	−0.14	−0.10 (2)	−0.09
113	−0.12 (2)	−0.13	−0.08 (2)	−0.09

(1995), assuming a room-temperature lattice parameter of 3.524 Å. The final column shows the averaged values obtained using our ZAPMATCH analysis. Considerable disagreement exists between the previous solid-state-theory results of Wang & Callaway (1977) (calculated at room temperature) and Wakoh & Yamashita (1971) (calculated at 0 K and converted to room temperature allowing for the lattice-parameter change) and the X-ray measurements of Diana *et al.* (1969). The later electron diffraction CV results of Fox & Fisher (1988) have been re-analysed to correct for an erroneous Debye–Waller factor used in the original analysis. The CV results now show excellent agreement with those of Wang & Callaway (1977).

The latest solid-state-theory values (from *WIEN*95) and the ZAPMATCH refinements are also in good agreement with the Wang & Callaway (1977) and critical-voltage results. Though both experiments use an electron beam, the natures of the experiments are radically different, with the CV measurements relying on *relative* intensity measurements to determine the voltage at which a systematic degeneracy occurs, while the ZAPMATCH technique us based on an *absolute* intensity pattern-matching approach. The self-consistency of the four sets of structure factors demonstrates the validity of both the theoretical methods and the two independent experimental techniques. This experimental confirmation of the accuracy of the theoretical calculations is reassuring as so much weight is currently given to the use of solid-state theories in the solution of many materials problems. Conversely, these results also provide further proof of the accuracy of the ZAPMATCH quantitative CBED technique.

The equivalent liquid-nitrogen results are shown in Table 4. In this case, our comparison with other results is restricted to the *WIEN*95 solid-state-theory calculations and critical-voltage values. The former have been recalculated with a lattice parameter of 3.517 Å. The latter have been rescaled assuming that the charge distribution remains unchanged and that the only difference from room temperature is the change in lattice parameter. Again, the agreement between the three sets of results is very good. The ZAPMATCH results, which have been obtained from liquid-nitrogen data, behave in the same manner as the recalculated *WIEN*95 values and the rescaled CV data, indicating that the differences observed between our room-temperature and liquid-nitrogen results arise mainly from the change in lattice parameter and not from any temperature-dependent redistribution of the bond charge.

The X-ray structure factors presented in Tables 3 and 4 are obtained from the real part of the electron scattering potential in our refinement calculations. How do the imaginary components of the electron structure factors behave for these fits? Can any information be extracted from them? The sensitivity results given in Tables 1 and 2 clearly indicate that we are able to refine the imaginary terms as part of the fit. Table 5 shows a comparison of the averaged best-fit imaginary electron structure factors (in Å^{-2}) with the equivalent values as given by the Einstein model (Bird & King, 1990). At both temperatures, the refined structure factors behave in a consistent manner. Similar to the values predicted by the Einstein model, all of the refined results are negative and decay as a function of the scattering angle. However, in both cases the magnitudes of the lowest-

Table 6. *Comparison of ZAPMATCH measurements of liquid-nitrogen-temperature copper structure factors (e atom^{-1}) with previous experimental results*

		X-ray	γ-ray	Critical voltage			
g	Neutral-atom values	Takama & Sato (1982)	Schneider *et al.* (1981)	Humphreys (1975)	Thomas *et al.* (1974)	Smart & Humphreys (1980)	ZAPMATCH (average)
111	22.05	21.77 (6)	21.51 (5)	21.75 (3)	21.70 (2)	21.76	21.78 (2)
200	20.70	20.25 (11)	20.22 (4)	20.43 (4)	20.42 (2)	20.43	20.44 (2)
220	16.75	16.72 (8)	16.45 (5)	16.71 (14)†	16.71 (14)†	16.68	16.72 (11)
113	14.75	14.71 (4)	14.54 (4)	–	–	–	14.78 (13)

† Value from Rocher & Jouffrey (1972).

Table 7. *Comparison of liquid-nitrogen-temperature copper structure factors (e atom^{-1}) obtained from various solid-state-theory calculations*

The final column shows the average of the theory results in columns 3–5.

g	Neutral atom	Bagayoko *et al.* (1980)	Wakoh & Yamashita (1971)	*WIEN*95	Average
111	22.05	21.68	21.69	21.71	21.69
200	20.70	20.35	20.43	20.37	20.38
220	16.75	16.62	16.60	16.66	16.63
113	14.75	14.70	14.61	14.75	14.69

order structure factors are increased by ~30% over the Einstein value with an increased decay rate returning the fitted values to the Einstein level for the {220} and {113} structure factors. Thus, while the Einstein model provides a reasonable description of the behaviour of the imaginary structure-factor components, it is clear that we are able to extract more accurate information regarding the TDS correction factors directly from the ZAPMATCH refinements.

5. Structure-factor measurements for copper

The same analysis procedures have been applied to ⟨110⟩ zone-axis data acquired from a polycrystalline copper foil at liquid-nitrogen temperatures. In this case, we have considered three patterns ranging in thickness from 900 to 3100 Å, each with a refined Debye–Waller factor of 0.21 Å^2 [see the paper by Saunders *et al.* (1999) for details of the Debye–Waller factor analysis]. The refinement calculations include 103 beams exactly and an additional 264 *via* Bethe potentials. Again, the refinement data set is restricted to intensities from the reflections out to {200}.

Previous reviews of structure-factor measurements and calculations for copper, such as that given by Mackenzie & Mathieson (1992), have demonstrated the widespread disagreement that exists between the variety of experimental and theoretical techniques that have been used. A summary of some of the more consistent experimental and theoretical structure-factor values is given in Tables 6 and 7. The experimental results include the X-ray *Pendellösung* results of Takama & Sato (1982), the γ-ray measurements of Schneider *et al.* (1981), three alternative sets of critical-voltage values [determined by Humphreys (1975) and Thomas *et al.* (1974), with the {220} value from Rocher & Jouffrey (1972), and the results of Smart & Humphreys (1980)] and the ZAPMATCH results averaged over the three data sets. Table 7 gives a comparison of the previous solid-state-theory calculations of Bagayoko *et al.* (1980) and Wakoh & Yamashita (1971) with the results we have obtained using the *WIEN*95 package. The final column shows the average theory result. It should be noted that, where the calculations or measurements were carried out at room temperature, they have been rescaled to liquid-nitrogen temperatures, allowing only for the change in the lattice parameter. As with the nickel results, of the previous experimental measurements, it is the electron diffraction critical-voltage values that are in best agreement with theory. However, this time the critical-voltage results lie consistently above the comparable theory values. The X-ray measurements of Takama & Sato (1982) are also in reasonable agreement, except for their {200} value, which is well below that predicted by theory.

The agreement between the ZAPMATCH results and the solid-state-theory calculations that we observed for nickel is not repeated for copper. The ZAPMATCH structure-factor values are consistently higher than their theory counterparts. Comparing our results with the previous experimental data, however, provides for much greater optimism. It is immediately apparent that the γ-ray measurements of Schneider *et al.* (1981) show agreement with neither the other experimental measurements given in Table 6 nor the theory results in Table 7. However, except for the {200} value of Takama & Sato (1982), which, as we have already observed, seems unusually low, and the {111} value of Thomas *et al.* (1974), which shows good agreement with the theory values, there is excellent agreement between the other experimental measurements and our ZAPMATCH results. It is unlikely that three different experimental techniques could suffer from the same systematic errors. Thus, the copper structure-factor results suggest that the disparity between theory and experiment may arise

Table 8. *Comparison of ZAPMATCH measurements of TDS imaginary electron structure factors ($Å^{-2}$) for liquid-nitrogen-cooled copper with those given by the Einstein model*

g	ZAPMATCH	Einstein model
111	−0.15 (1)	−0.11
200	−0.14 (1)	−0.11
220	−0.12 (1)	−0.10
113	−0.10 (2)	−0.10

from problems with the theoretical calculations rather than errors in the experimental measurements.

The imaginary TDS structure-factor corrections for these calculations are presented in Table 8. As with the nickel data described in the previous section, we observe that the best-fit imaginary components are negative and decay as a function of the scattering angle in a similar manner to the Einstein model values. In addition, we again find that the lowest-order terms increase in magnitude and that an increased decay rate returns them to Einstein values after three or four terms. It is interesting to note that the {111} correction is increased by ∼30% compared with its Einstein model value, which is consistent with the change noted for both the room-temperature and liquid-nitrogen nickel data. Thus, these copper results are a further indication that we are able to refine the imaginary structure-factor contributions in addition to the real (charge-density-dependent) potential.

6. Second-order TDS corrections

We have seen how the ZAPMATCH and critical-voltage results for nickel agree within standard uncertainties. In addition, the CV results of Humphreys (1975) and the corresponding ZAPMATCH analysis are also in agreement for copper. However, in both cases, the {111} and {200} structure factors obtained from the ZAPMATCH analysis are found to be slightly higher. Thus, the question arises as to whether this difference has a systematic explanation or is merely a random effect.

It has been shown by Anstis (1996) that the Einstein model that we have already used to provide estimates of the imaginary TDS correction factors can also be used to determine second-order corrections which alter the real part of the scattering potential. These corrections are considerably smaller than their imaginary counterparts but could be sufficient to explain the deviation of our results from the critical-voltage values. The corrections are voltage dependent and decrease as a function of the incident-beam energy. Thus, at the higher voltages required for CV measurements, the corrections should be insignificant. However, in his paper, Anstis (1996) suggested that the accuracy with which ZAPMATCH can make low-order structure-factor measurements may be sufficient to detect these second-order TDS corrections at the accelerating voltages used in our experiments, *i.e.* ∼200 kV.

We have therefore repeated our calculations, including the second-order corrections to the real part of the scattering potential as given by computer programs supplied to us by Dr Geoff Anstis of the University of Technology, Sydney, Australia. This alters the analysis in two ways. First, each of the higher-order structure factors that remains fixed at its neutral-atom value during the fit is modified to include the second-order TDS corrections. Second, the best-fit structure factors are corrected for the effects of the TDS modifications before they are converted to X-ray structure factors for comparison with previous measurements.

The results of the repeated analysis of the room-temperature nickel data and liquid-nitrogen copper data are shown in Tables 9 and 10. The original ZAPMATCH results (without the second-order TDS corrections) are shown in column 3. Columns 4 and 5 give two alternative versions of the TDS-corrected analysis. The values given in column 4 correspond to the use of the second-order TDS corrections as supplied by the Anstis programs. Those listed in column 5 have been obtained by multiplying the real (second-order) corrections by the same factors by which the first-order (imaginary) terms were measured to increase, *e.g.* the {111} correction increased by ∼30% and the {200} increased by ∼10–20%. It is apparent from these results that the use of second-order TDS corrections could provide an explanation of the differences between the ZAPMATCH and CV measurements. However, given the small effects of the corrections, it is difficult to state categorically that this is the true cause of the difference.

7. Discussion

The development of quantitative CBED techniques such as ZAPMATCH and the close-to systematic approach of Spence & Zuo (1992) has given new impetus to the experimental measurement of bonding effects in crystals. The accuracy achieved by these techniques rivals the optimum performance of previous experimental techniques based on X-ray and γ-ray diffraction. However, the small probe sizes associated with the CBED methods (around a few nanometres) enable this accuracy to be achieved across a much wider range of materials for which the other techniques are severely limited by sample imperfections. The most accurate structure-factor measurements made previously employed the critical-voltage method (Fox & Fisher, 1988). The applicability of this technique is limited, however, by its requirement for a high-voltage microscope. Thus, the introduction of quantitative CBED techniques using conventional TEMs is a major advance in the experimental determination of structure factors. The proliferation of solid-state-theory calculations has suggested a new application for the experi-

Table 9. *Comparison of room-temperature nickel structure factors (e atom^{-1}) obtained from solid-state-theory calculations, critical-voltage measurements, ZAPMATCH and ZAPMATCH with TDS corrections*

g	Solid-state theory (average)	CV (Fox &Fisher, 1988)	ZAPMATCH standard analysis	ZAPMATCH with TDS corrections	ZAPMATCH with scaled TDS corrections
111	20.45	20.45 (1)	20.47 (2)	20.45 (2)	20.44 (2)
200	19.12	19.12 (2)	19.13 (2)	19.12 (2)	19.11 (2)
220	15.46	–	15.43 (8)	15.43 (4)	15.42 (4)
113	13.64	–	13.67 (8)	13.66 (8)	13.66 (8)

Table 10. *Comparison of liquid-nitrogen-temperature copper-structure factors (e atom^{-1}) obtained from solid-state-theory calculations, critical-voltage measurements, ZAPMATCH and ZAPMATCH with TDS corrections*

g	Solid-state theory (average)	CV (Smart & Humphreys, 1980)	ZAPMATCH standard analysis	ZAPMATCH with TDS corrections	ZAPMATCH with scaled TDS corrections
111	21.69	21.76	21.78 (2)	21.77 (2)	21.76 (2)
200	20.38	20.43	20.44 (2)	20.42 (2)	20.41 (2)
220	16.61	16.68	16.72 (11)	16.70 (10)	16.69 (10)
113	14.69	–	14.78 (13)	14.78 (12)	14.78 (12)

mental techniques, *i.e.* by making sufficiently accurate experimental measurements can we test the validity of the various theoretical approaches?

The metals nickel and copper provide an ideal demonstration of the difficulties associated with comparing diverse experimental and theoretical results. Many attempts have been made to determine the charge distributions in these materials by using a range of experimental and theory techniques. However, the reviews presented by Wang & Callaway (1977) for nickel and Mackenzie & Mathieson (1992) for copper show the considerable disparity that exists between the alternative methods. The addition of our ZAPMATCH analysis and theory calculations using the *WIEN*95 FLAPW code of Blaha *et al.* (1995) allow us to draw more definitive conclusions based on the consensus between the low-order structure-factor values obtained with the different techniques.

The nickel ZAPMATCH results (Tables 3 and 4) are within standard uncertainties of the critical-voltage measurements reported by Fox & Fisher (1988), which were considered to be the most accurate experimental measurements made previously for this material. In addition, both experiments are in agreement with the *WIEN*95 FLAPW calculations and those of Wang & Callaway (1977). This consistency must be considered evidence of the accuracy of both experiment and theory when applied to nickel. This reassuring situation is not repeated for copper, however, for which the experimental and theory results are found to be *separately* consistent, *i.e.* the ZAPMATCH results agree with other experiments, while the *WIEN*95 calculations agree with other theories, but the agreement of theory with experiment is not as good. In this case, the consistency of the results obtained from radically different experimental techniques suggests that the source of the experiment–theory disparity possibly lies in some limitation of the theory rather than in systematic errors in the experiments.

The agreement between the ZAPMATCH results obtained from CBED patterns acquired at different sample thicknesses has been improved by introducing easily applied rules relating the sensitivity of CBED patterns to the various low-order structure factors contributing to the diffraction contrast in the zone-axis patterns. Applying these rules, it has been possible to refine the imaginary correction potential that is introduced into CBED simulations to account for the effects of thermal diffuse scattering. It is conventional to calculate this correction potential using the Einstein model of independent atoms. Comparing the refined values of the potential with the Einstein predictions (Tables 5 and 8) shows that, while the model is adequate to describe most of the behaviour of the low-order structure-factor corrections, it consistently underestimates the magnitude of the corrections. For example, the {111} structure-factor correction in our room-temperature nickel and liquid-nitrogen-cooled nickel and copper deviates from the Einstein model value by $\sim$30% in each case. These results may have important consequences for other electron microscopy simulation techniques, such as those used in quantitative high-resolution electron microscopy (HREM) analysis where the limited accuracy of TDS correction methods has been proposed as a possible source of the problems encountered when trying to make quantitative comparisons of theory and experiment (Van Dyck, 1997).

The Einstein model also predicts additional correction terms which are small and have generally been ignored. At the accuracies reported for ZAPMATCH calculations, however, it is possible that the effects of these higher-order corrections will be detectable [as suggested by Anstis (1996)]. We have tested this hypothesis by repeating our structure-factor refinements while including the second-order (real) correction potential. The results (Tables 9 and 10) show that including the second-order corrections does bring the {111} structure factors obtained from the ZAPMATCH

analysis more into line with the critical-voltage measurements. Given that the structure-factor values only change by an amount equivalent to the error in the original measurement, however, this does not constitute proof that the corrections are necessary or correct. Further experiments are required using lower incident-beam energies or materials of higher atomic number, where the corrections would be more significant, before we can resolve this matter incontrovertibly.

In conclusion, the nickel and copper results presented here are further evidence of the rapid development under way in the field of quantitative CBED. The experimental accuracy that can now be achieved appears capable of testing the latest solid-state-theory calculations. In this case, we have shown that, while there is good agreement between theory and experiment for nickel, the results are less satisfactory for copper, possibly highlighting inaccuracies in the theory. The additional refinements to the ZAPMATCH technique discussed here demonstrate how the accuracy of the low-order structure-factor measurements can be improved by carefully considering the sensitivity of the data to the various structure factors. In addition, we are now in a position to investigate the effects of TDS corrections by refining the imaginary correction potential and testing the validity of using additional higher-order corrections obtained using the Einstein model.

This work was performed while one of the authors (MS) held a National Research Council Naval Post-graduate School Research Associateship, and another (PAM) held a Royal Society University Research Fellowship. The authors would like to thank Dr Geoff Anstis for making available computer codes for evaluating the TDS correction terms to the elastic scattering factors and for providing invaluable advice on their use, Dr Roger Vincent for his help during our time at Bristol, and Tim Walsh for providing the TEM samples.

References

Anstis, G. R. (1996). *Acta Cryst.* A**52**, 450–455.
Bagayoko, D., Laurent, D. G., Singhal, S. P. & Callaway, J. (1980). *Phys. Lett. A*, **76**, 187–190.
Bird, D. M. & King, Q. A. (1990). *Acta Cryst.* A**46**, 202–208.
Bird, D. M. & Saunders, M. (1992). *Ultramicroscopy*, **45**, 241–251.
Blaha, P., Schwarz, K., Dufek, K. & Augustyn, R. (1995). *WIEN*95. Technical University of Vienna 1995. [Improved and updated Unix version of the original copyrighted *XIEN* code published by P. Blaha, K. Schwarz, P. Sorantin, & S. B. Trickey (1990). *Comput. Phys. Commun.* **59**, 399.]
Diana, M., Mazzone, G. & DeMarco, J. J. (1969). *Phys. Rev.* **187**, 973–978.
Doyle, P. A. & Turner, P. S. (1968). *Acta Cryst.* A**24**, 390–397.
Fox, A. G. & Fisher, R. M. (1988). *Aust. J. Phys.* **41**, 461–468.
Holmestad, R., Mornirolli, J.-P., Zuo, J. M. & Spence, J. M. (1997). *Microsc. Microanal.* **3** (Suppl. 2), 1051–1052.
Holmestad, R., Zuo, J. M., Spence, J. C. H., Hoier, R. & Horita, Z. (1995). *Philos. Mag.* A**72**, 579–601.
Humphreys, C. J. (1975). *Rep. Prog. Phys.* **42**, 1825–1887.
Kossel, W. & MÎllenstedt, G. (1938). *Ann. Phys. (Leipzig)*, **36**, 113–119.
Mackenzie, J. K. & Mathieson, A. McL. (1992). *Acta Cryst.* A**48**, 231–236.
Rocher, A. M. & Jouffrey, B. (1972). *Electron Microscopy 1972. Inst. Phys. Conf. Ser.* No. 14, pp. 528–529. London/Bristol: The Institute of Physics.
Saunders, M., Bird, D. M., Zaluzec, N. J., Burgess, W. G., Preston, A. R. & Humphreys, C. J. (1995). *Ultramicroscopy*, **60**, 311–323.
Saunders, M., Fox, A. G. & Midgley, P. A. (1999). *Acta Cryst.* A**55**. 480–488.
Saunders, M., Midgley, P. A., Walsh, T. D., Menon, E. S. K., Fox, A. G. & Vincent, R. (1999). *Scanning Microsc.* Suppl. 11. In the press.
Schneider, J. R., Hansen, N. K. & Kretschmer, H. (1981). *Acta Cryst.* A**37**, 711–722.
Smart, D. J. & Humphreys, C. J. (1980). *Electron Microscopy and Analysis 1979. Inst. Phys. Conf. Ser.* No. 52C, ch. 4, pp. 528–529. London/Bristol: The Institute of Physics.
Spence, J. C. H. & Zuo, J. M. (1992). *Electron Microdiffraction*. New York: Plenum.
Takama, T. & Sato, S. (1982). *Philos. Mag.* B**45**, 615–626.
Tanaka, M. (1989). *J. Electron Microsc. Tech.* **13**, 27–39.
Thomas, L. E., Shirley, C. G., Lally, J. S. & Fisher, R. M. (1974). *High Voltage Electron Microscopy*, pp. 38–47. London/New York: Academic Press.
Van Dyck, D. (1997). *Microsc. Microanal.* **3**, (Suppl. 2), 1139–1140.
Wakoh, S. & Yamashita, J. (1971). *J. Phys. Soc. Jpn*, **30**, 422–427.
Wang, C. S. & Callaway, J. (1977). *Phys. Rev. B*, **15**, 298–306.
Zuo, J. M. (1992). *Ultramicroscopy*, **41**, 211–223.